Pet.Sci.(2014)11:550-562
DOI 10.1007/s12182-013-0371-0

Progression of injectivity damage with oily waste water in linear flow

Jin Lu[1]* and Wojtanowicz Andrew K[2]

[1] InPetro Technologies Inc., 9800 Centre Parkway, #860, Houston, TX 77036, USA
[2] Craft & Hawkins Department of Petroleum Engineering, Louisiana State University, Patrick F. Taylor Hall, Room 2160B, Baton Rouge, LA 70803, USA

Abstract: Numerous laboratory experiments and field cases show that even very small amount of oil in injected water can cause severe injectivity damage. Although injectivity decline caused by oil droplets has been studied experimentally, there is still lack of an easy-to-use and widely accepted model to predict the decline behavior. In this work, we developed an analytical model to predict the time-dependent progress of the water permeability reduction in linear flow by analyzing experimental data obtained from linear core flooding.

The model considers mass transfer of the oil phase from the produced water to the rock due capture effects by dispersion, advection and adsorption inside the rock. As the captured oil saturation increases, permeability reduces following the relative permeability drainage relationship. The reduction stabilizes when the oil saturation comes to an equilibrium value controlled by oil droplet size and injection velocity. The model is calibrated using published experimental data from prolonged core floods with oil-contaminated waste water. Theoretical runs of the model replicate all the effects known from experimental observations. Resulting from the model is a distributed change of permeability vs. time and distance from the point of injection that can be converted to the overall injectivity damage.

Key words: Produced water injection, injectivity decline, permeability damage, linear flow model, filtration model

1 Introduction

Currently, produced water becomes the single largest waste generated in the petroleum industry in the U.S (Veil and Clark, 2009). Produced water reinjection (PWRI) is now recognized as an important way to address this problem, as it protects environment while improving oil production (Abou-Sayed et al, 2007; Rousseau et al, 2008; Buret et al, 2010, Jin and Wojtanowicz, 2011). Although PWRI is attractive from both environmental and economic points of view, great uncertainties still remain about the consequences of the process and the actual injectivity behavior (Veil and Quinn, 2004; Rousseau et al, 2008). Field practice shows that, injectivity declines continuously in PWRI process and many wells require fracturing to maintain the target injection rates (King and Adegbesan, 1997; Detienne et al, 2002; 2005; Hustedt et al, 2008). Both experimental and theoretical work has shown that even a tiny amount of oil in water can cause severe formation damage around injectors by oil droplet capture, especially when there is no oil saturation in the formation at the beginning of injection (McAuliffe, 1973a; Soo and Radke, 1984a;, 1986; Rege and Fogler, 1988; Zhang et al, 1993; Ohen, et al, 1996; Bennion et al, 1998; Civan, 2007; Buret et al, 2010). Thus it is important to understand and mathematically describe how oil capture and flow blockage develops at and away from the rock face.

Although, much work has been done and many models are available to predict the injectivity decline caused by solid particles, there is a lack of easy-to-use models to predict the injectivity damage caused by oil contamination in the injection water (Pang and Sharma, 1997; Al-Riyamy and Sharma, 2004; Vaz et al, 2006; Buret et al, 2010). Soo and his partners carried out experimental and theoretical work to study emulsion flow behavior in porous media. They found that the capture of oil droplets in rock is similar to that of solid colloids during a deep bed filtration process (Schmidt et al, 1984; Soo and Radke, 1984a; 1984b, 1986; Soo et al, 1986). Thus, droplet capture, that is, mass transfer between the liquid globule and the solid matrix, is analogous to the traditional solid particle filtration theory. The two main capture mechanisms at work are: straining, where oil droplets clog the pore throats as shown in Fig. 1, and interception — with droplets captured by van der Waals colloidal forces. For emulsions, there is usually a distribution of droplet sizes, so straining would dominate the large droplet capture while

*Corresponding author. email: lujin329@yahoo.com
Received August 20, 2013

interception would contribute primarily to small droplet capture. Usually, it is probably sufficient to assume a uniform droplet size distribution, and the capture parameters employed would then reflect combined straining and interception modes (Soo and Radke, 1984a; 1984b, 1986; Cosse, 1993; Auset and Keller, 2006; Buret et al, 2010).

The purpose of this study is to build a simple analytical model for injectivity decline caused by invasion of oil droplets and their adsorption in porous media. By using the mass balance principle we can derive governing equations for oil mass transfer from oily water to the rock matrix, resulting from various droplet capture mechanisms. The model shall describe oil saturation increase in the rock space, and define the maximum (equilibrium) oil saturation based on droplet to pore throat size ratio and the capillary number. The oil saturation change should give permeability reduction described by the relative permeability relationship. The results of the model have been verified with the published data of different authors.

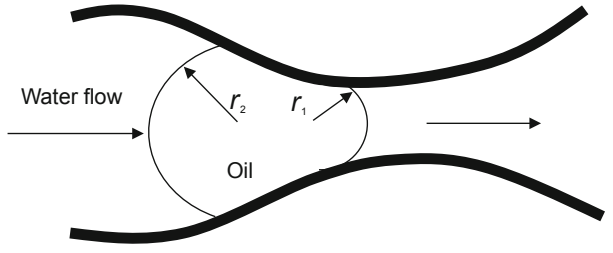

Fig. 1 Oil droplet flows through a restricted pore throat

2 Mathematical model of oil droplet transport and adsorption in porous media

2.1 Mechanisms of oil droplet trapping and re-suspension

McAuliffe (1973a; 1973b) studied the mechanisms of oil droplets flowing through porous media, where he considered a single droplet entering a pore throat smaller than the droplet size as shown in Fig. 1. The capillary pressure is greater at the front of the droplet than at its back, and a certain pressure is required to force the droplet through the pore throat, i.e. the viscous force should be greater than the capillary force on the droplet, otherwise, the oil droplet will be trapped. This phenomenon has been recognized as the main reason for the permeability reduction in the oily water injection process (Mendez, 1999). When the oil droplets are much smaller than the pore throat, they may still be captured by van der Waals colloidal forces and accumulated on the surface of the pores, which reduces the effective flow path of water and causes water permeability reduction (Auset and Keller, 2006; Buret et al, 2010). Oil saturation in the porous media increases with the trapping process going on. Mathematically, this phenomenon can be modeled by a retention (or adsorption) process according to previous studies (Barone et al, 1992; Johnson and Elimelech, 1995; Borden, 2007; Clayton and Borden, 2009).

The pressure differential required to mobilize a macro droplet through a pore throat can be characterized by the capillary number, which is defined as the ratio of viscous to capillary forces. The mobilization of residual oil usually begins at a capillary number of about 10^{-5} for water-wet rocks (Lake, 1989). For typical water injection conditions, the capillary number in the reservoir is around 10^{-7} and only a limited area around the injector has a capillary number greater than 10^{-5} (Mendez, 1999). Thus, the trapped oil may re-enter the flowing water under certain circumstances. As a result, the oily water injection is a dynamic process of oil droplet trapping and re-suspension, which indicates the mathematical model should consider both oil droplet adsorption and desorption. In our model, the desorption effect is implicitly included in oil saturation and capillary number relationship, which will be described in details in the following sections.

2.2 Basic assumptions

Similar to Moghadasi, Soo and their coworkers' study, the mathematical expressions derived in this work are based on the following assumptions (Soo and Radke, 1984a; 1984b; 1986; Soo et al, 1986; Moghadasi et al, 2004):

The rock is consolidated and homogeneous, no fines migration happens in the injection process.

1) The oil droplets and pore throats are log-normally distributed;

2) Oil droplets are the only contaminant, there are no solid particles in the injection water;

3) Oil droplets are stable and their sizes are constant in the water before being injected into the core;

4) The oily water is injected into the core at a constant flow rate;

5) No oil is generated or lost in the process.

To establish a mathematical model for predicting oil droplet transport and capture in porous media, three mechanisms are considered: 1) advection due to velocity, 2) dispersion caused by molecular transport, concentration gradients and external force fields (mechanical mixing, turbulent diffusion, etc.) —described by Fick's Law, and 3) adsorption induced by straining and interception captures and desorption caused by high capillary number as described above. In one-dimensional flow, the oil transport to the porous media can be expressed as:

Advection rate (m_a): $m_a = uCA$

Dispersion rate (m_d) (Fick's Law): $m_d = -D\left(\partial C / \partial x\right) A$

Dynamics of oil droplet trapping and re-suspension:

$$\frac{\partial S_o}{\partial t} = \alpha\left(1 - \frac{S_o}{S_{oe}}\right) C$$

where u is the interstitial water velocity, which is equal to the Darcy velocity divided by the porosity, m/s; C is the mass concentration of oil in water, kg/m^3; A is the cross-section area, m^2; D is the overall dispersion coefficient which includes the effects of molecular transport, concentration gradient, mechanical aspects, etc., m^2/s; S_o is the mass saturation of oil trapped in the rock, which can be easily transferred to volume saturation by dividing by the oil density, kg/m^3; α is the adsorption coefficient which represents the ability of rock to trap oil droplets, s^{-1}; S_{oe} is the equilibrium oil saturation in the

rock, kg/m^3.

The oil adsorption rate is related to the oil concentration in water and the equilibrium oil saturation in the rock. Higher oil concentration means more oil in water and the matrix has a higher probability of capturing oil droplets, thus the oil saturation increases faster. The equilibrium oil saturation is a function of velocity, which will be discussed in detail later. Usually, higher velocity leads to lower equilibrium oil saturation due to a high capillary number, which reduces the oil adsorption rate. The adsorption stops when the oil saturation in the rock reaches the equilibrium value. Thus, the dynamics of oil adsorption and desorption are implicitly included in the oil saturation and capillary number relationship. A detailed description can be found in the "Equilibrium oil saturation" section.

The total amount of oil transported parallel to the flow direction is obtained by summing the mass transported by advection and dispersion. Thus, the total amount of mass transported to a controlled volume is:

$$m = \phi u C - \phi D \frac{\partial C}{\partial x} \tag{1}$$

The mass change in the controlled volume is:

$$\Delta m = -\frac{\partial m}{\partial x} \mathrm{d}x \tag{2}$$

Because there is no loss of oil in the process, the difference between the amount of oil entering and leaving the controlled volume must be equal to the amount of oil accumulated in the element, part of it is trapped in the rock matrix and part of it is remaining in water in the controlled volume. So, the rate of mass change can be expressed as:

$$\Delta m = \left[\phi \frac{\partial C}{\partial t} + (1-\phi) \frac{\partial S_\mathrm{o}}{\partial t} \right] \mathrm{d}x \tag{3}$$

where m is mass, kg; ϕ is the porosity of the porous media, fraction. Combining Eqs. (1), (2) and (3) gives a one dimensional continuity equation for oily water flowing through porous media:

$$D \frac{\partial^2 C}{\partial x^2} - u \frac{\partial C}{\partial x} = \frac{\partial C}{\partial t} + \frac{(1-\phi)}{\phi} \frac{\partial S_\mathrm{o}}{\partial t} \tag{4}$$

Most experiments are carried out under flow conditions, where the velocity effect is much stronger than the dispersion effect, i.e. the flow is in the advection-dominated region. In this region, the transportation mechanism of immiscible fluids is similar to that of miscible fluids (Perkins and Johnston, 1963; 1969; Duan, 2009; Jha et al, 2011).

To solve Eq. (4), "$\partial S_\mathrm{o}/\partial t$" should be transformed to an expression of "$\partial C/\partial t$" to obtain an analytical solution. Based on the Langmuir adsorption equation, the adsorbed oil saturation can be solved by the following equation (Satter et al, 1980):

$$S_\mathrm{o} = \left[1 - \exp\left(-\frac{\alpha t C}{S_\mathrm{oe}}\right) \right] S_\mathrm{oe} \tag{5}$$

where α is the adsorption coefficient, s^{-1}.

Notice that both time and oil concentration are variables in Eq. (5). Usually it is helpful to reduce the number of variables to make the process analysis more clear. Studies of the kinetics of adsorption often assume a simple relationship between oil saturation (S_o) and oil concentration (C) at low oil concentration, as the adsorption process mainly depends on concentration rather than time, and the concentration is a function of time itself which includes the time effect already. The reason is that, when the oil concentration is low, the number of oil droplets is much less than that of pores in the rock. Oil droplets are caught quickly by pores with similar or smaller sizes in the clean aquifer until all the available capturing sites are filled, i.e. the equilibrium oil saturation is reached (Schmidt et al, 1984). According to the discussion by Satter et al (1980), Eq. (5) can be simplified as Eq. (6) when the system reaches an equilibrium condition. The simplification is also adopted by commercial reservoir simulators such as CMG® (McKee and Swailes, 1991; CMG, 2011; Xu et al, 2013).

$$S_\mathrm{o} = \frac{\alpha S_\mathrm{oe} C}{1 + \alpha C} \tag{6}$$

However, Eq. (6) contains strongly nonlinear items after transformation as shown in Eq. (7), which is difficult to solve analytically when substituting into Eq. (4):

$$\frac{\partial S_\mathrm{o}}{\partial t} = \left[\frac{\alpha S_\mathrm{oe}}{1+\alpha C} - \frac{\alpha^2 S_\mathrm{oe} C}{(1+\alpha C)^2} \right] \frac{\partial C}{\partial t} \tag{7}$$

When the oil concentration is low, i.e. the value of C is small, the oil adsorption rate in the matrix is proportional to the rate of change of the oil concentration in water. Thus, the following relationship is valid and could be used to solve Eq. (4) analytically (Marino, 1974; Satter et al, 1980; Yadava et al, 1990):

$$\frac{\partial S_\mathrm{o}}{\partial t} = \beta \frac{\partial C}{\partial t} \tag{8}$$

where β is a parameter related to the oil adsorption process, dimensionless. Using Eq. (8), $\partial S_\mathrm{o}/\partial t$ is eliminated from Eq. (4) and the distributed oil concentration vs. time and distance can be determined by solving Eq. (4) with one initial and two boundary conditions. We assume an infinite linear injection zone and define the following initial and boundary conditions:

Initial conditions, there is no oil in the core before injection:

$$S_\mathrm{o} = C = 0 \qquad \text{at } t = 0,\ x > 0 \tag{9}$$

Inner boundary conditions, the oil concentration is constant in the injection water before entering the core:

$$C = C_\mathrm{o} \qquad \text{at } t > 0,\ x = 0 \tag{10}$$

Outer boundary conditions, there is no oil in the core at infinite length:

$$S_\mathrm{o} = C = 0 \qquad \text{at } t > 0,\ x \to \infty \tag{11}$$

Solution to Eq. (4) gives the oil concentration profile in

water:

$$C=\frac{C_o}{2}\left\{erfc\left(\frac{Rx-ut}{\sqrt{4DRt}}\right)+\exp\left(\frac{ux}{D}\right)erfc\left(\frac{Rx+ut}{\sqrt{4DRt}}\right)\right\} \quad (12)$$

with

$$R=1+\frac{\beta(1-\phi)}{\phi} \quad (13)$$

where *erfc*() is the complementary error function

The dimensionless parameter R —also called retention factor— represents the interaction between oil droplets and rock. Its higher value means more oil droplets contact the grains and are captured faster, which leads to higher oil saturation in the pore space (Gupta and Greenkorn, 1974; Rege and Fogler, 1988).

In the actual evaluation of Eq. (12), the term $\exp(ux/D)$ is large while the term $erfc\left[(Rx+ut)/\sqrt{4DRt}\right]$ becomes very small for large values of argument —orders of magnitude smaller than the term $\exp(ux/D)$, so their product can be ignored. For example, only the first and second terms are considered in Eq. (12) to match laboratory results under various conditions (Brigham, 1974).

When the oil concentration profile is known, the oil saturation change in the rock can be determined using Eq. (6). Following this approach and by substituting Eqs. (12) and (13) into Eq. (6), we obtain the oil saturation distribution in the rock and oil concentration (by mass) in water as:

$$\begin{cases} C=\dfrac{C_o}{2}erfc\left(\dfrac{Rx-ut}{\sqrt{4DRt}}\right) \\ S_o=\dfrac{\alpha S_{oe}C_o erfc\left(\dfrac{Rx-ut}{\sqrt{4DRt}}\right)}{\rho_o\left[2+\alpha C_o erfc\left(\dfrac{Rx-ut}{\sqrt{4DRt}}\right)\right]} \\ R=1+\dfrac{\beta(1-\phi)}{\phi} \end{cases} \quad (14)$$

2.3 Equilibrium oil saturation

Equilibrium oil saturation is defined here as the asymptotic maximum value of oil saturation in the core that would not increase with continuing injection of the same oily water at a constant rate. It is a function of the ratio of the droplet diameter to the pore-throat diameter and the capillary number as shown in Eqs. (15) and (16), respectively:

$$N_d=\frac{d_o}{d_{pt}} \quad (15)$$

$$N_{Ca}=\frac{\mu_w u}{\sigma_{ow}}=\frac{\mu_w q}{A\phi\sigma_{ow}} \quad (16)$$

where N_d is the ratio of the droplet diameter to the pore-throat diameter (we will call it "size ratio" for short in the following text), dimensionless; d_o is the average diameter of oil droplets, μm; d_{pt} is the average pore-throat diameter, μm; N_{Ca} is the capillary number —the ratio of viscous to capillary force, dimensionless; μ_w is the water viscosity, cP; u is the interstitial velocity, m/s; q is the injection rate, m^3/s; A is the rock cross section area, m^2; ϕ is the porosity of the porous media; σ_{ow} is the oil-water interfacial tension, dyne/cm.

There are many different definitions of the capillary number in the literature. For example, some authors define N_{Ca} using superficial (filtration or Darcy) velocity while others use interstitial velocity to represent the viscous effect. Although these capillary numbers have the same physical meaning, one should be careful to use them as their effective validity regions are different (Hilfer and Øren, 1996). For example, for a core sample with porosity of 0.1, the value of "critical" capillary number defined below using the superficial velocity is 10^{-5} but the one with the interstitial velocity gives 10^{-4}. As the capillary number plays an important role in this study, we discuss it further in the following sections (Chatzis and Morrow, 1984; Schlumberger, 2007).

$$N_{Ca}^*=\frac{\mu_w u_c}{\sigma_{ow}} \quad (17)$$

where u_c is the critical velocity required to reduce the residual oil in the rock, m/s. Currently, there is no widely accepted formula to calculate the equilibrium oil saturation from the oil droplet size (Schmidt et al, 1984; Soo and Radke, 1984a; 1984b; Rege and Fogler, 1988; Buret et al, 2010; Romero et al, 2011). Based on the experimental results and discussion in various publications, we can develop a correlation to estimate the value of equilibrium oil saturation, S_{oe}.

Most of laboratory experiments have been carried out under low-velocity conditions with low capillary number ($N_{Ca}<10^{-4}$) representing the actual field injection scenario. For example, if an injection well with the following parameters: 0.3 ft radius, 20 ft completion length, 0.5 cP water viscosity and 50 dyne/cm oil water interfacial tension, is injecting water at 5000 barrels per day (bpd) to a disposal formation with 0.3 porosity, the capillary number is 8.8×10^{-5}. Experiments conducted within this range of capillary number for different cores and fluids have shown that the equilibrium oil saturation mainly depends on the ratio of the oil droplet diameter to the pore-throat diameter with little effect of velocity (Schmidt et al, 1984; Soo and Radke, 1984a; 1984b, 1986; Soo et al, 1986; Buret et al, 2008; 2010). Using the data from these experiments, we make a semi-log plot shown in Fig. 2. The

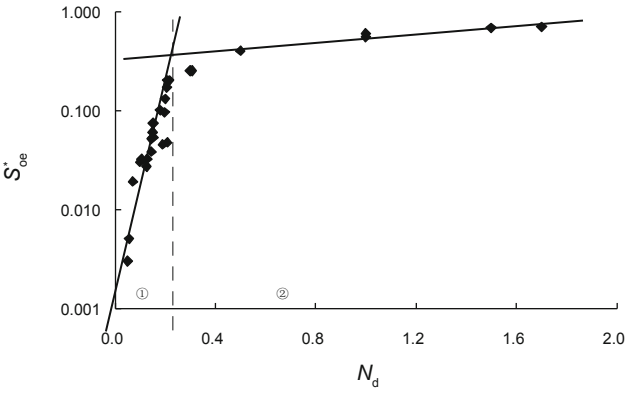

Fig. 2 Equilibrium oil saturation changes with the ratio of the droplet diameter to the pore-throat diameter in a low capillary number region

plot comprises two regions of the relationship between S^*_{eo} (equilibrium oil saturation at a low capillary number region) vs. N_d (the size ratio): the "interception" capture (N_d<0.25) and "straining" capture (N_d>0.25) regions – described above.

In the interception capture region, the oil saturation increases fast with the size ratio. This is because, initially, oil droplets move freely in large pores and are preferentially captured in the small size pores. As the injection proceeds, more and more of the small pores become blocked. This blockage leads to a flow diversion toward even larger pores and the rate of small oil droplet capture decreases until an equilibrium saturation is reached and no more capture occurs.

In the straining capture region, the equilibrium oil saturation is always high and changes slowly with respect to the size ratio. One explanation is that the big oil droplets block the pore throats by lodging between sand grains, either a single droplet or several droplets bridged together. If the pressure gradients are not enough to overcome the capillary resistance between the grains and droplets, the flow path is plugged and no other droplets can pass it.

When the flow velocity is high (typically N_{Ca}>10^{-4}), the equilibrium oil saturation decreases rapidly with respect to the capillary number as shown in Fig. 3 (Soo and Radke, 1984b). In this region, the viscous force is much greater than the capillary force, which makes the strained droplets squeeze through or break up and pass the pore throats. This phenomenon has been confirmed by other researchers who also suggested exponential decrease in the equilibrium oil saturation in this region (Rege and Fogler, 1988; Romero et al, 2011).

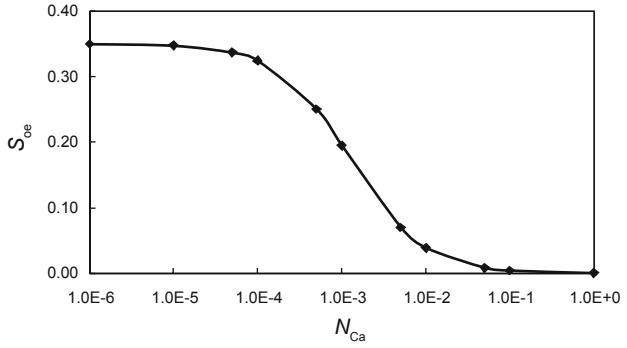

Fig. 3 Equilibrium oil saturation changes with capillary number (d_o/d_{pt} = 1.5)

Various correlations have been developed to predict the residual oil saturation based on the capillary number for the routine core analysis, which is known as the capillary desaturation process. Due to physical analogy between residual oil saturation and the equilibrium oil saturation postulated in this study, we use the residual oil saturation correlation to relate the equilibrium oil saturation changing with capillary number. Eq. (18) is such a relationship used in a commercial numerical simulator for N_{Ca}<1, to predict residual oil saturation when the "bump rate" testing data is not available (Schlumberger, 2007):

$$S_{oe} = S^*_{oe}\left[1-\exp\left(-\lambda\frac{N^*_{Ca}}{N_{Ca}}\right)\right] \tag{18}$$

where S_{oe} is the equilibrium oil saturation at a certain capillary number, dimensionless; S^*_{oe} is the maximum equilibrium oil saturation under a low capillary number condition, which is determined by the routine core analysis, dimensionless; λ is an empirical constant experimentally determined from the bump rate tests, dimensionless; N^*_{Ca} is the critical capillary number when the equilibrium oil saturation begins to decrease, dimensionless. Substantially different capillary desaturation curves are obtained for different types of rock in the literature. The shape of the curve depends largely on the pore size distribution in the porous medium and fluids properties (Foster, 1973; Morrow and Chatzis, 1984; Lake, 1989; Sheng, 2011). In most cases, there is no clarity on the values of critical capillary number from laboratory data and it may vary from 10^{-6} to 10^{-4} for different rocks. The precise value needs to be determined experimentally for each combination of rock and fluids (Morrow et al, 1988; Lake, 1989; Hilfer and Øren, 1996; Hirasaki et al, 2006; Sheng, 2011).

2.4 Bump rate test for trapped oil mobilization

Usually, the trapped oil mobilization in a core can be determined from a "bump rate" test, which directly shows the oil saturation and water relative permeability changing with respect to the capillary number. We use the following example to show the typical "bump rate" test for a core from the Entrada Formation with 2.47 cm in diameter and 5.11 cm in length: when the water injection rate increases from 3 cm^3/min to the bump rate, 6 cm^3/min, more oil (7.7%) is produced and the water relative permeability increases significantly, from 0.206 to 0.368 as shown in Fig. 4. The S_{oe} = 0.215 obtained from the bump rate seems to be useful as a significant increase in oil production is observed. When the viscous force is much greater than the capillary force, the residual oil saturation can be further lowered to 0.15 which means the trapped oil is displaced with an increase in capillary number.

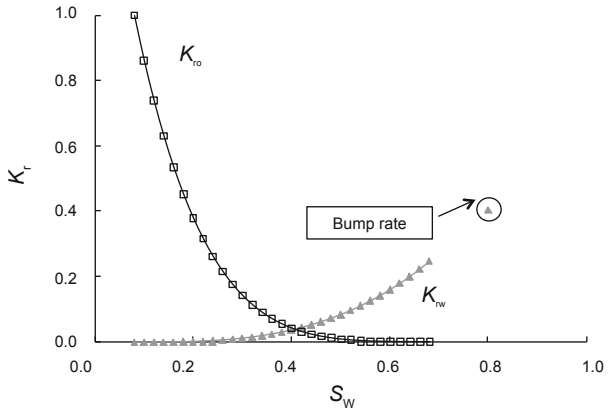

Fig. 4 Relative permeability curves from the "bump rate" test

Based on oil droplet trapping mechanisms, we can define different oil droplet capture regions for different combinations of capillary number and size ratio values as shown in Fig. 5. To find the equilibrium oil saturation in Eq. (5), we need to know the size ratio to determine S^*_{oe} from Fig. 2. Then, we

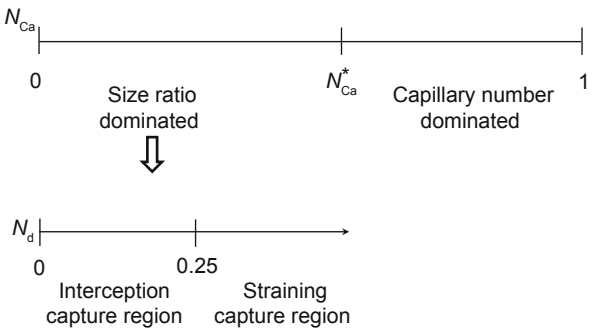

Fig. 5 Oil droplet capture regions for combinations of capillary number and size ratio

use Eqs. (16) and (18) to calculate S_{oe} for the known injection rate and interstitial velocity.

2.5 Injectivity decline prediction

Distribution of oil saturation with distance can be used to determine the degree of damage to water injectivity caused by the oil content. For two-phase (oil and water) flow through porous media, we can use relative permeability theory to estimate the injectivity decline (Devereux, 1974a; 1974b; Spielman and Su, 1977; Ohen et al, 1996; Bennion et al, 1998; Civan, 2007). Using the relative permeability concept (Schramm, 1992), the water injectivity in linear flow can be expressed as:

$$I_w = \frac{q_w}{\Delta p} = \frac{10^{-6} K_w A}{\mu_w \Delta L} = \frac{10^{-6} K K_{rw} A}{\mu_w \Delta L} \tag{19}$$

where I_w is the water injectivity index, $m^3/s/kPa$; q_w is the water injection rate, m^3/s; Δp is the pressure drop through the core, kPa; K_w is the effective water permeability, D; K is the absolute permeability of the core, D; K_{rw} is the relative permeability to water, fraction; A is the cross section area of the core, m^2; ΔL is the length of the core, m. As only K_{rw} changes during the injection process, the water injectivity decline as a function of time can be calculated from Eq. (20) (Saripalli et al, 2000):

$$I_D = \frac{I_{w\_t}}{I_{w\_0}} = \frac{K_{w\_t}}{K_{w\_0}} = \frac{K_{rw\_t}}{K_{rw\_0}} \tag{20}$$

where I_D is the dimensionless injectivity decline index, and subscripts 0 and t denote initial and instant values, respectively. Relative permeability values can be obtained in various ways. If the core data are not available, Corey's function might be used to approximate the relative permeability to water at different oil saturations (Brooks and Corey, 1966):

$$K_{rw} = K^*_{rw} \left(\frac{1 - S_o - S_{wc}}{1 - S_{or} - S_{wc}} \right)^{n_w} \tag{21}$$

where K^*_{rw} is the relative permeability to water at residual oil saturation, fraction; S_{wc} is the connate water saturation, fraction; S_{or} is the residual oil saturation, fraction; n_w is the exponent for water relative permeability, dimensionless.

When oily water is injected into a clean aquifer with no initial oil saturation, i.e. S_o=0 at t=0, $K^*_{rw} \equiv 1$ and $S_{or} \equiv 0$, the water relative permeability becomes:

$$K_{rw} = \left(\frac{1 - S_o - S_{wc}}{1 - S_{wc}} \right)^{n_w} \tag{22}$$

Eq. (22) is valid for $0 \le S_o \le S_{oe}$. As shown in Fig. 6, the effect of oil capture on injectivity damage changes considerably for different rock and fluid properties. Oil would not flow for oil saturation below the equilibrium oil saturation, S_{oe}. Since the S_{oe} value depends on flow velocity, it could be much smaller than the typical value of residual oil saturation from standard core testing (Brooks and Corey, 1966; Ramakrishnan and Wasan, 1984; Huang et al, 1997). Moreover, the water injectivity would decline at different rates (exponent n_w) in different formations. Usually n_w was lower in oil wet rocks than in water wet rocks (Schramm, 1992). It follows that, the water injectivity would decline slowly in oil wet aquifers that are not very common. If the core testing data are available, the water relative permeability (drainage cycle) curve should be used, as the oil droplets invasion process is a water drainage process (Huang et al, 1997).

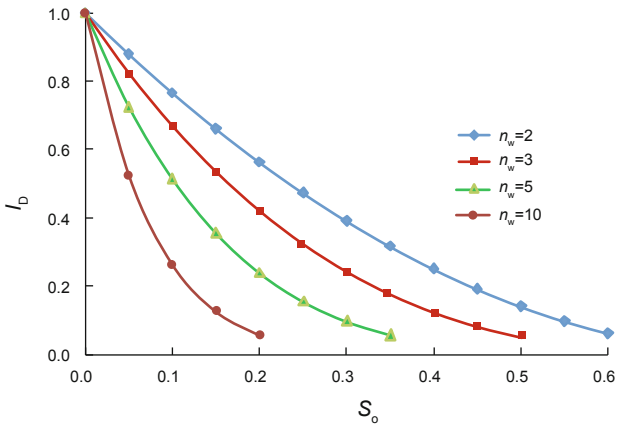

Fig. 6 Shape of water injectivity decline curves

3 Model verification

From the mathematical model derived above, we are able to predict the changes of oil concentration in water, oil saturation in the pore space and water permeability with time and distance during the injection process. In the following sections, we use published data to verify the model. If the model is valid for all of them, then we can use it to predict the phenomena that are difficult to measure experimentally, such as the oil concentration in water at a specified location of the core, oil saturation distribution in the core in the injection process.

3.1 Oil concentration change with time and distance

Table 1 shows the experimental data reported from injection experiments and parameters used to match the effluent oil concentration. Soo and Radke (1984a) carried out experiments using Ottawa sand packs to investigate the emulsion flow behavior in porous media. They kept the oil concentration in the injection water at 5,000 ppm while

changing droplet size to evaluate the effect of size ratio on permeability decline. They measured the effluent oil concentration as shown in Fig. 7. It is clear that, the size ratio plays an important role when the emulsion flows through the sand pack. A higher size ratio delays the oil breakthrough time which indicates that big oil droplets are captured more easily in the rock than the small ones. Buret et al (2010) confirmed this phenomenon by varying both size ratio and inflow oil concentration as shown in Fig. 8. Again, the model matches the results very well for different cases.

Table 1 Experimental runs for effluent concentration measurement

Parameter	Soo and Radke, 1984a			Buret et al, 2010	
	Case 1	Case 2	Case 3	Case 1	Case 2
Core	Ottawa sand pack	Ottawa sand pack	Ottawa sand pack	SiC pack	SiC pack
Core length L, m	0.05	0.05	0.05	0.1	0.1
Core diameter d, m	0.025	0.025	0.025	0.0152	0.0152
Porosity ϕ	0.34	0.34	0.34	0.40	0.45
Flow velocity u, m/s	4×10^{-5}	4×10^{-5}	4×10^{-5}	3.77×10^{-5}	3.77×10^{-5}
Size ratio N_d	0.071	0.105	0.152	0.020	0.100
Oil concentration C_o, ppm	5000	5000	5000	82	129
Dispersion coefficient D, m^2/s	1.0×10^{-6}	2.0×10^{-7}	1.5×10^{-7}	5.0×10^{-7}	3×10^{-7}
Adsorption constant β	1.3	3.0	7.0	100	400

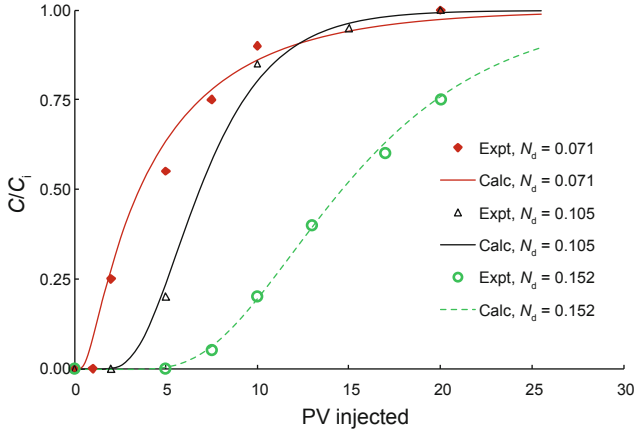

Fig. 7 Comparison of calculated and measured effluent oil concentrations at different size ratios. Experimental results are from Soo and Radke (1984a).

Only the effluent oil concentration change with time was measured in the experiments. It is difficult to determine spatial distribution of oil concentration in water throughout the core, so no concentration distribution has been reported in the literature. However, using the model, it is possible to describe the oil concentration and saturation change with location in the rock. The calculated spatial distribution of oil concentration in water at any time is shown in Figs. 9 and 10. The fast decrease in the oil concentration with distance shown in the figures indicates that a significant amount of oil is retained in the rock when the oily water flows through it, which is to be discussed in the next section.

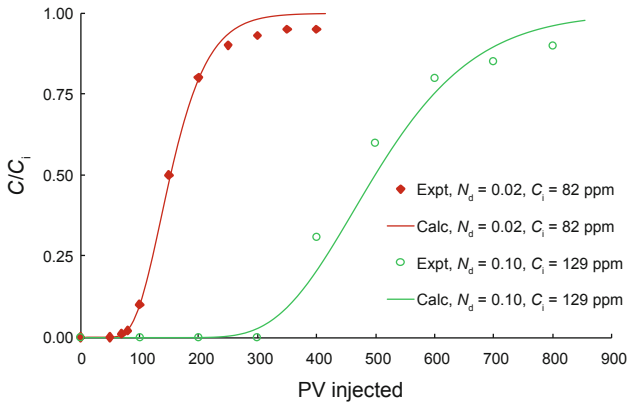

Fig. 8 Comparison of calculated and measured effluent oil concentrations at various size ratio and influent oil concentrations. Experimental results are from Buret et al (2010).

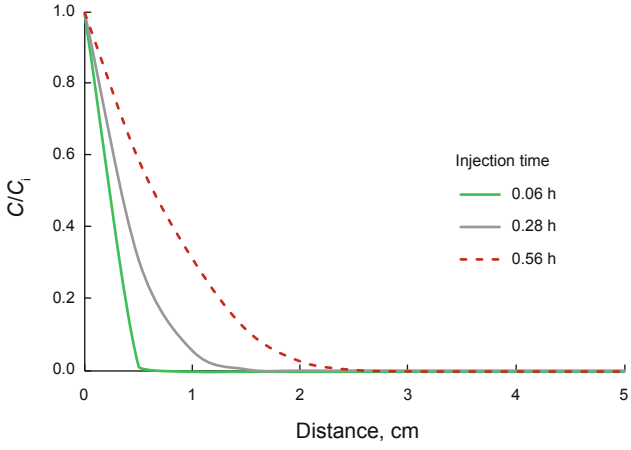

Fig. 9 Predicted oil concentration vs. distance after matching Soo and Radke's experiments (1984a)

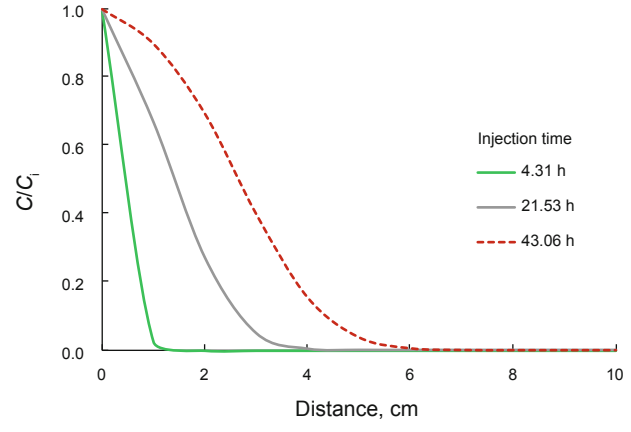

Fig. 10 Predicted oil concentration vs. distance after matching Buret et al's experiments (2010)

3.2 Oil saturation change with time and distance

Oil saturation development and distribution in the rock sample are the key factors to understand the injectivity impairment process during oily water injection (Devereux, 1974a; 1974b; Spielman and Su, 1977; Schramm, 1992; Ohen et al, 1996; Bennion et al, 1998; Civan, 2007). However,

similar to the oil concentration in water, no oil saturation change along the core samples have been reported from oily water injection experiments. Using the model developed in this study, we are able to predict the oil saturation distribution in the core at any location and time as shown in Figs. 11 and 12, respectively. From these figures, it is clear that oil captured in the rock reduces with distance from the rock face. The trend clearly corresponds to the predicted oil concentration change with distance in Figs. 9 and 10. However, all these predictions are merely theoretical and require some verification.

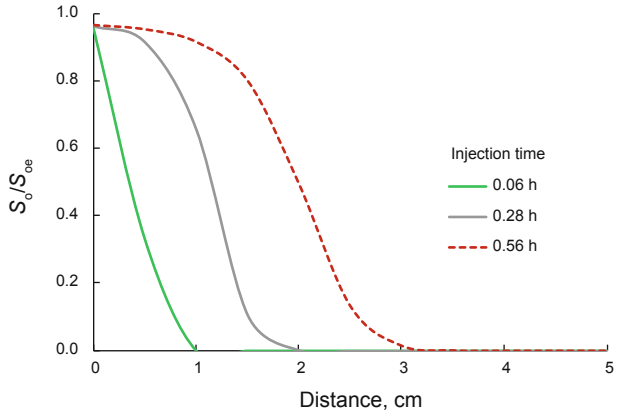

Fig. 11 Predicted distribution of oil saturation in the core at different times after matching Soo and Radke's experiments (1984a)

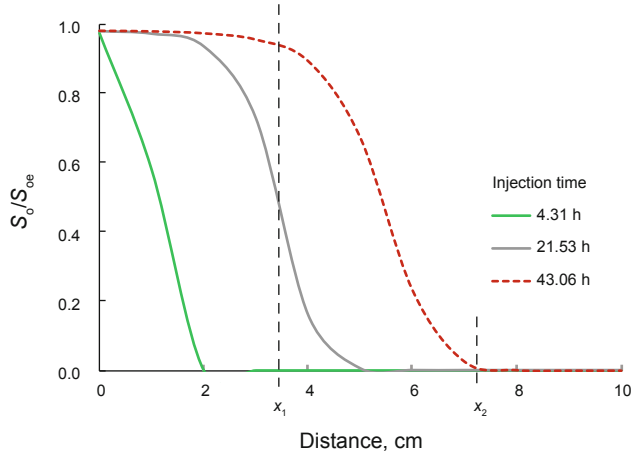

Fig. 12 Predicted distribution of oil saturation in the core at different times after matching Buret et al's experiments (2010)

As there were no experimental data available for the oil saturation distribution in the core, we built a one-dimensional simulation model using the commercial reservoir simulator STARS of CMG®, to verify and visually observe the dilute oily water flowing through the core. We used Buret et al's data and built the model as shown in Fig. 13. In the model, each grid has a length of 0.5 cm in the horizontal direction, 0.27 cm in the vertical direction with 1.345 cm width. The initial oil saturation in the core was set equal to zero and the oily water was injected from left to right. Fig. 14 shows the advance of the oil front with saturation distribution matching that in Fig. 12. The distribution shows expansion of the maximum-damage zone ($S_o = S_{oe}$) proceeded with a relatively short frontal zone (from x_1 to x_2) with oil saturation dropping from S_{oe} to zero.

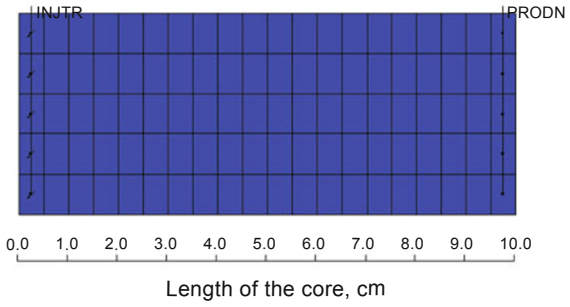

Fig. 13 Cross-section view of simulation model for oily water injection to a core

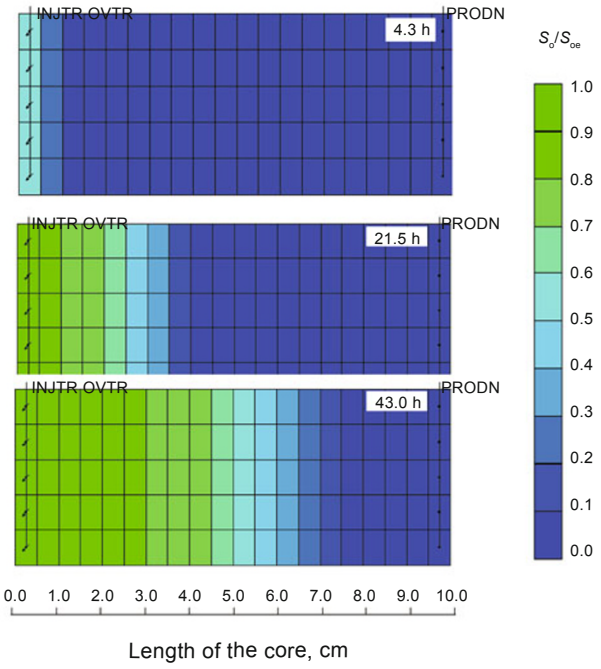

Fig. 14 Simulated advance of oil front during oily water injection in Buret et al's experiments (2010)

3.3 Water permeability damage

In core flooding experiments, the expanding oil saturation might be expressed as distributed permeability damage in the core (Soo and Radke, 1984b; Soo et al, 1986; Zhang et al, 1993; Ohen et al, 1996; Buret et al, 2010). The conversion is made using the fractional flow concept and the relative permeability relationship. For the oil front zone, the average oil saturation is:

$$S_{o\_avg} = \frac{\int_{x_1}^{x_2} S_o(x)\,dx}{\Delta x} \tag{23}$$

where $\Delta x = x_2 - x_1$ is the size of oil front zone, m; S_{o_avg} is the average oil saturation in the zone, fraction; and $S_o(x)$ is the function of oil saturation distribution. By considering the relative permeability relationship, $K_{rw} = \phi(S_o)$, similar to Eq. (22), we can calculate the average relative permeability of the

advancing oil front (from x_1 to x_2) as:

$$K_{\mathrm{rw\_avg}} = \frac{\Delta x}{\int_{x_1}^{x_2} \frac{1}{K_{\mathrm{rw}}(x)} \mathrm{d}x} \tag{24}$$

where the water relative permeability is a function of oil saturation:

$$K_{\mathrm{rw}}(x) = \phi\left[S_{\mathrm{o}}(x)\right] \tag{25}$$

For the core injection experiments we may have discrete measurements of the pressure drop over the length of the core as shown in Fig. 15. In such case, we may compute a series of permeabilities in the core sections as:

$$K_{\mathrm{w}i} = \frac{10^6 q \mu_{\mathrm{w}} L_i}{A \Delta p_i} \tag{26}$$

Or the average permeability as:

$$K_{\mathrm{w\_avg}} = \frac{10^6 q \mu_{\mathrm{w}} L_{\mathrm{t}}}{A} \frac{1}{\sum_{i=1}^{n} \Delta p_i} \tag{27}$$

where L_i is the length of each section, m; L_{t} is the total length of the core, m; A is the cross-section area of the core, m^2; q is the flow rate through the core, m^3/s; Δp_i is the pressure drop in a subsection, kPa; $K_{\mathrm{w}i}$ is the water permeability of a subsection, D; $K_{\mathrm{w\_avg}}$ is the average water permeability over the core section, D; i is the subsection number; and n is the total subsection number over the core. The above equations show that a thin section with low permeability could significantly reduce the average core permeability.

In order to use the theoretical model and verify results from the published core floods, some input data must be inferred from the results. Typically, the relative permeability data are not reported from experiments and they can be estimated using the core permeability and oil saturation data. This approach becomes also useful for reducing the number of experiments as we only need to carry out part of the experimental work to get several data points and predict the whole set of injectivity curves based on these data.

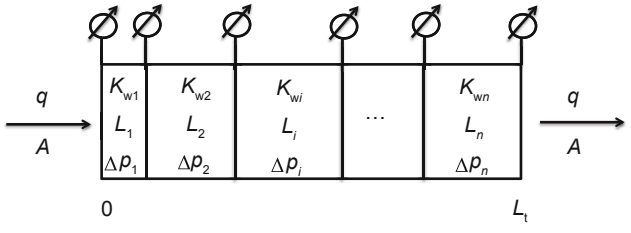

Fig. 15 Local and average water permeability over a core

Generally, for a given rock and fluid, the dispersion coefficient value, D, is small and could be treated as a constant in some cases, especially when the flow is in the low capillary number region. Adsorption coefficients, α or β increase with the size ratio and the oil concentration as oil droplets have a higher probability to be captured, and decrease with the capillary number as oil droplets may deform and squeeze through the pore throats when the viscous force is high. Also they have less time to contact a rock section and their probability of being captured becomes lower (Coats and Smith, 1964; Gupta and Greenkorn, 1974; Rege and Fogler, 1988).

Fig. 16 shows the water injectivity reduction in different sections of the core measured and calculated with the model. For the model input, we used values of model constants from Table 1 and the fractional flow function shown in the following equation for Case 1 reported by Buret et al (2010):

$$K_{\mathrm{w}}(S_{\mathrm{o}}) = 2490(1 - S_{\mathrm{o}})^{12.5} \tag{28}$$

where $K_{\mathrm{rw}}^{*} = 1$, $S_{\mathrm{wc}} = 0$, $S_{\mathrm{or}} = 0$ as the sand pack is made with clean SiC without connate water and residual oil.

As some coefficients used in the model were not reported, we calibrated the model by matching history data from experimental results by using following procedure:

First, we used the model to fit the reported values of oil concentration change vs. time at the core exit to find parameters D and β. For example, in Fig. 8, we matched the effluent oil concentration for two cases reported by Buret et al (2010) with D and β shown in Table 1.

Next, we predicted the oil concentration change vs. distance at different times as shown in Fig. 10.

Then, we inferred the fractional flow relationship using the reported I_{D} in the first section of the core as shown by the black solid line in Fig. 16. The adsorption coefficient (α) and exponent for water relative permeability (n_{w}) could be determined.

Finally, we used the fractional flow relationship to predict the I_{D} change in other sections based on the previously computed D, β, α and n_{w}, and verified the predictions with reported data as shown by the red solid and green black dash lines in Fig. 16.

When all of the coefficients are determined, the linear model can be transformed to a radial flow model for describing the real well situation as discussed by Bear (1972), Duan (2009), and shown by Jin (2013).

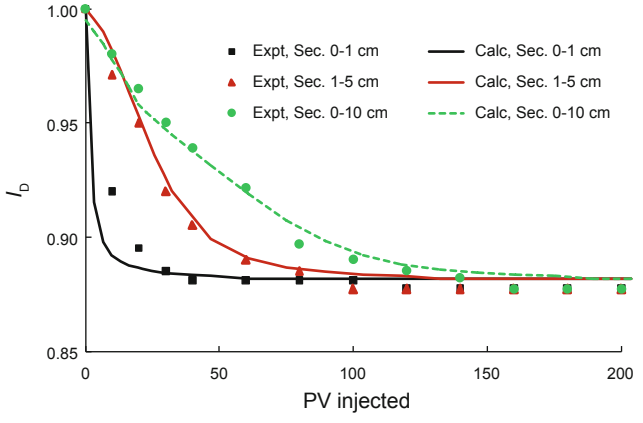

Fig. 16 Calculated and measured water injectivity damage in different core sections —data from Buret et al (2010)

A very good match indicates the validation of the model. From Fig. 16 we can see that, even for the low size ratio (0.02) and low oil concentration (82 ppm), there is still about 13% permeability loss of the core. The most severe

damage happens in the first section (0-1 cm) of the core at the beginning of injection. However, if the injection continues, the whole core will be damaged. This observation confirms the situation discussed in Figs. 12 and 14. If the core flooding does not last long enough to reach the final equilibrium condition, the first section will be found to be damaged severely while the other sections have less or no damage as shown in Fig. 17, which is also experimentally confirmed by other researchers (Zhang et al, 1993; Ohen et al, 1996). This effect is more obvious for higher size ratios as shown in Fig. 18. The water permeability in the first section reduces to 0.2 and 0.1 of the original value when the size ratios are 1 and 1.67, respectively (Buret et al, 2010).

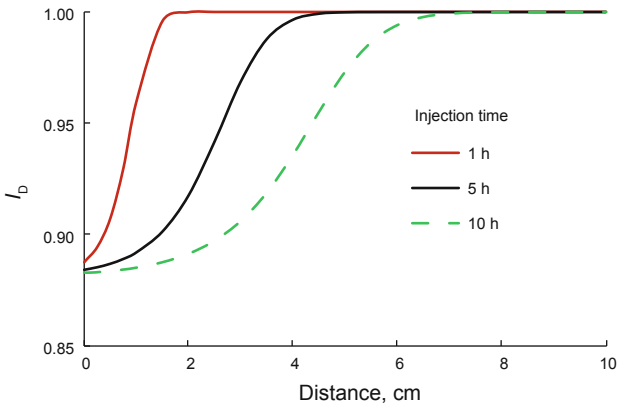

Fig. 17 Calculated spatial distribution of water injectivity damage in the core at different injection times —experimental data from Buret, et al (2010)

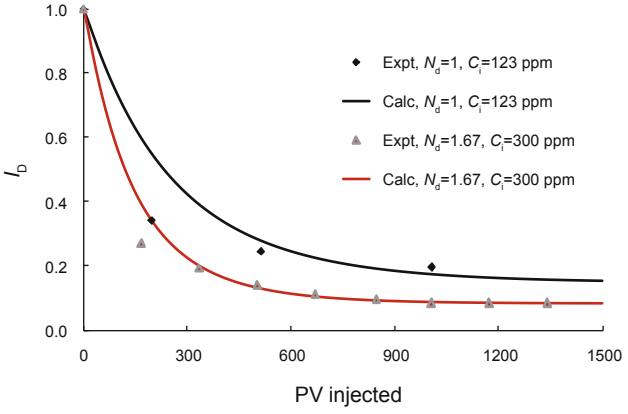

Fig. 18 Calculated and measured water injectivity reduction in the first section (0-1 cm) of the core —experimental data from Buret et al (2010)

Fig. 19 clearly shows the effect of size ratio on injectivity decline for the same core: a size ratio of 0.071 causes about a 20% injectivity decline while a size ratio of 0.152 makes the core lose 75% of its water permeability. It also indicates that a higher oil concentration gives equilibrium sooner (Zhang et al, 1993). Notice that, the size ratios in Fig. 19 are quite low, from 0.071 to 0.152, but the water permeability reduces faster than other cases. The reason might be that the core used in Fig. 19 is strongly water wet, as we use higher value of n_w (= 15) to match the results, which indicates the core is strongly water wet while the cores used by Zhang et al (1993) are likely to have been neutral or slightly oil wet ($n_w \approx 2$). This indicates that oil wet formations are better candidates for water injection than water wet ones, which has been confirmed by both the laboratory research and field tests (Wang et al, 2010; Ju et al, 2012).

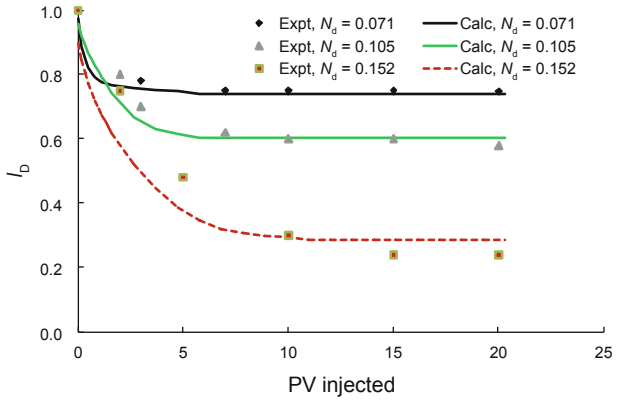

Fig. 19 Size ratio effect on water injectivity reduction from model and experiments with a constant oil concentration —experimental data from Soo and Radke (1984a)

Most researchers in the oily water injection area addressed the flow in the low capillary number region, where the velocity effect is small. However, the effect of velocity could not be ignored for water flow at high capillary number where the viscous force effect becomes significant (Soo and Radke, 1984b; Rege and Fogler, 1988; Romero et al, 2011). Soo and Radke (1984b) carried out experiments to investigate the velocity effect, where 10,000 ppm oily water with a size ratio of 1.5 was injected to a core at capillary number from 10^{-5} to 10^{-2} as shown in Fig. 20. The model's output confirms the injectivity damage for capillary number exceeding 10^{-4}, while there is almost no damage when the N_{Ca} value approaches 10^{-2}. Thus, the model correctly simulates the physical effect observed in experiments. The physical reason may be that oil droplets break up into very small ones at a high velocity, and the viscous force is much greater than the capillary force which makes the droplets deform easily to pass through the pore throats. Also, it takes a much shorter time for the droplets to travel through a rock section so that the residence

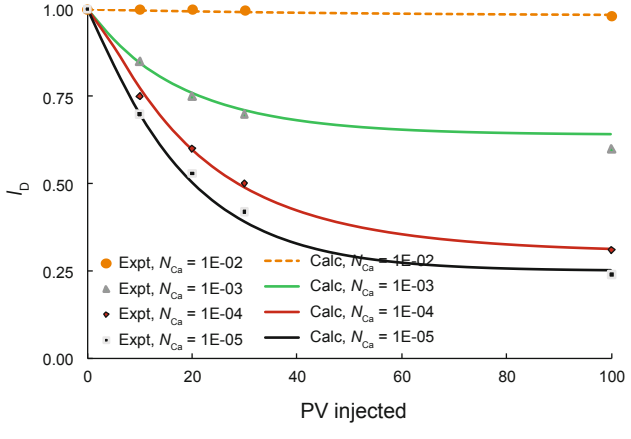

Fig. 20 Effect of capillary number on water injectivity decline

time is too short for the rock surface to adsorb the droplets, i.e. the probability of droplets to be captured is greatly reduced when they flow through the rock at a very high velocity. However, only a small region near a real well could reach a high capillary number when the well is operated at a high rate.

In the model, we address the N_{Ca} effect by including it in S_{oe} as shown in Eq. (18). S_{oe} decreases rapidly with N_{Ca} in a high capillary number region as shown in Fig. 3 (Soo and Radke, 1984b). From the relative permeability relationship shown in Eq. (21), it is clear that low equilibrium oil saturation gives high water relative permeability, which means small water injectivity damage.

4 Conclusions

Although water injectivity decline caused by solid particles has been widely studied, there are few models for predicting injectivity damage due to oily water – particularly with very low oil content. This study introduces an analytical model to explain injectivity decline caused by spatial advance of water permeability damage over time. The model is derived from the mass balance of oil phase while considering the effects of oil droplet transport and capture due to combined effects of advection, dispersion and adsorption coupled with the two phase relative permeability relationship. The model was studied and verified using experimental data from published experiments. The study leads to the following conclusions:

1) The proposed model was verified using published experiments showing good matches and replicating reported observations.

2) The model can be calibrated by matching results from standard laboratory injection with oil-contaminated water and rock cores. The match can be improved with relative permeability and bump rate testing.

3) A simulation model is built to visually observe the oil saturation front moving in the core. The simulator output confirms the results from the analytical model in terms of local permeability damage along the core.

4) The model replicates experimental observation that a very low oil content in injected water does not reduce the ultimate damage but merely delays the development of oil saturation in the rock.

5) The model reproduces the oil droplet to pore size ratio effect on injectivity damage. The effect is represented by the correlation of equilibrium oil saturation and oil droplet to pore size ratio. Oil saturation reaches equilibrium condition faster for large oil droplets.

6) The model demonstrates the rock wettability effect by showing that injectivity damage with oily water is more severe in water wet formations than in oil wet rocks. The wettability effect is implicit in the model through the fractional flow relationship.

7) The effect of injection rate on injectivity damage is included in the model through the correlation of capillary number and equilibrium oil saturation. The injection rate has a slight effect when the capillary number is less than 10^{-4}, however, it can significantly improve the injectivity when it becomes greater than 10^{-4} in vicinity of the rock face.

8) The distance-averaged permeability —derived from the model— is a general indicator of injectivity loss and can be used to predict linear injectivity index change in time.

Acknowledgements

This study is part of a research program, Downhole Water Sink Technology Initiative (DWSTI) —a Joint Industry Project (JIP) at LSU. Authors would like to express their appreciation to the JIP members for supporting this work.

References

Abou-Sayed A S, Zaki K S, Wang G, et al. Produced water management strategy and water injection best practices: design, performance, and monitoring. SPE Production & Operations. 2007. 22(1): 59-68 (paper SPE 108238)

Al-Riyamy K and Sharma M M. Filtration properties of oil-in-water emulsions containing solids. SPE Drilling & Completion. 2004. 19(3): 164-172 (paper SPE 73769)

Auset M and Keller A. Pore-scale visualization of colloid straining and filtration in saturated porous media using micromodels. Water Resources Research. 2006. 42(12): 1-9

Barone F S, Rowe R K and Quigley R M. A laboratory estimation of diffusion and adsorption coefficients for several volatile organics in a natural clayey soil. Journal of Contaminant Hydrology. 1992. 10(3): 225-250

Bear J. Dynamics of Fluids in Porous Media. Elsevier Publishing Co., Inc. New York, 1972. 665-727

Bennion D B, Bennion D W and Thomas F B, et al. Injection water quality —a key factor to successful waterflooding. Journal of Canadian Petroleum Technology. 1998. 37(6): 53-62

Brigham W E. Mixing equations in short laboratory cores. SPE Journal. 1974. 14(1): 91-99 (paper SPE 4256)

Borden R C. Effective distribution of emulsified edible oil for enhanced anaerobic bioremediation. Journal of Contaminant Hydrology. 2007. 94(1-2): 1-12

Brooks R H and Corey A T. Properties of porous media affecting fluid flow. Journal of the Irrigation and Drainage Division. 1966. 92(2): 61-88

Buret S, Nabzar L and Jada A. Emulsion deposition in porous media: impact on well injectivity. Paper SPE 113821 presented at Europec/EAGE Conference and Exhibition, June 9-12, 2008, Rome, Italy

Buret S, Nabzar L and Jada A. Water quality and well injectivity: do residual oil-in-water emulsions matter? SPE Journal. 2010. 15(2): 557-568 (paper SPE 122060)

Chatzis I and Morrow N R. Correlation of capillary number relationships for sandstone. SPE Journal. 1984. 24(5): 555-562 (paper SPE 10114)

Civan F. Reservoir Formation Damage: Fundamentals, Modeling, Assessment, and Mitigation. 2nd edition. Elsevier: Gulf Professional Publishing, 2007

Clayton M H and Borden R C. Numerical modeling of emulsified oil distribution in heterogeneous aquifers. Ground Water. 2009. 47(2): 246-58

CMG. STARS User's Guide – Version 2011. Calgary: Computer Modelling Group Ltd., 2011

Coats K H and Smith B D. Dead-end pore volume and dispersion in porous media. SPE Journal. 1964. 4(1): 73-84 (paper SPE 647)

Cosse R. Basics of Reservoir Engineering: Oil and Gas Field Development Techniques. Paris: Editions Technip. 1993

Detienne J L, Danquigny Y and Lacourie M E. Produced water re-

injection on a low permeability carbonaceous reservoir. Paper SPE 78482 presented at Abu Dhabi International Petroleum Exhibition and Conference, Oct. 13-16, 2002, Abu Dhabi, United Arab Emirates

Detienne J L, Ochi J and Rivet P. A simulator for produced water re-injection in thermally fractured wells. Paper SPE 95021 presented at SPE European Formation Damage Conference, May 25-27, 2005, Scheveningen, The Netherlands

Devereux O F. Emulsion flow in porous solids: I. a flow model. The Chemical Engineering Journal. 1974a. 7(2): 121-128

Devereux O F. Emulsion flow in porous solids: II. experiments with a crude oil-in-water emulsion in porous sandstone. The Chemical Engineering Journal. 1974b. 7(2): 129-136

Duan S K. Progressive Water-oil Transition Zone due to Transverse Mixing Near Wells. Ph.D. Dissertation. Baton Rouge: Louisiana State University. 2009

Foster W R. A low-tension waterflooding process. Journal of Petroleum Technology. 1973. 25(2): 205-210 (paper SPE 3803)

Gupta S P and Greenkorn R A. Determination of dispersion and nonlinear adsorption parameters for flow in porous media. Water Resource Research. 1974. 10(4): 839-846

Hilfer R and Øren P E. Dimensional analysis of pore scale and field scale immiscible displacement. Transport in Porous Media. 1996. 22(1): 53-72

Hirasaki G J, Miller C A, Pope G A, et al. Surfactant based enhanced oil recovery and foam mobility control. Technical Report to DOE. 2006. DE-FC26-03NT15406

Huang D D, Honarpour M M and Al-Hussainy R. An improved model for relative permeability and capillary pressure incorporating wettability. Paper SCA 9718 presented at SCA International Symposium. Sep. 7-10, 1997, Calgary, Canada

Hustedt B, Zwarts D, Bjoerndal H P, et al. Induced fracturing in reservoir simulations: application of a new coupled simulator to a water flooding field example. SPE Reservoir Evaluation & Engineering. 2008. 11(3): 569-576 (paper SPE 102467)

Jha R K, Bryant, S and Lake, L W. Effect of diffusion on dispersion. SPE Journal. 2011. 16(01): 65-77 (paper SPE 115961)

Jin L and Wojtanowicz A K. Minimum produced water from oil wells with water-coning control and water-loop installations. Paper SPE 143715 presented at SPE Americas E & P Health, Safety, Security, and Environmental Conference, Mar. 21-23, 2011, Houston, Texas

Jin L. A Feasibility Study of Multi-functional Wells for Water Coning Control and Disposal. Ph.D. Dissertation. Baton Rouge: Louisiana State University, LA, Dec. 2013

Johnson P R and Elimelech M. Dynamics of colloid deposition in porous media: blocking based on random sequential adsorption. Langmuir. 1995. 11: 801-812

Ju B, Fan T, Li Z, et al. Improving water injectivity and enhancing oil recovery by wettability control using nanopowders. Journal of Petroleum Science and Engineering. 2012. 86-87: 206-216

King R W and Adegbesan K O. Resolution of the principal formation damage mechanisms causing injectivity and productivity impairment in the Pembina Cardium reservoir. Paper SPE 38870 presented at SPE Annual Technical Conference and Exhibition, Oct. 5-8, 1997, San Antonio, Texas

Lake L W. Enhanced Oil Recovery. New Jersey: Prentice Hall. 1989

Marino M A. Distribution of contaminants in porous media flow. Water Resources Research. 1974. 10(5): 1013-1018

McAuliffe C D. Oil-in-water emulsions and their flow properties in porous media. Journal of Petroleum Technology. 1973a. 25(6): 727-733 (paper SPE 4369)

McAuliffe C D. Crude-oil-water emulsions to improve fluid flow in an oil reservoir. Journal of Petroleum Technology. 1973b. 25(6): 721-726 (paper SPE 4370)

McKee S and Swailes D. On the derivation of the Langmuir isotherm for adsorption kinetics. Journal of Physics A: Mathematical and General. 1991. 24(4): L207

Mendez Z D C. Flow of Dilute Oil-in-water Emulsions in Porous Media. Ph.D. Dissertation. Austin, University of Texas at Austin, TX, Dec. 1999

Moghadasi J, Müller-Steinhagen H, Jamialahmadi M, et al. Theoretical and experimental study of particle movement and deposition in porous media during water injection. Journal of Petroleum Science and Engineering. 2004. 43(3-4): 163-181

Morr ow N R and Chatzis I. Measurement and correlation of conditions for entrapment and mobilization of residual oil. Final Report for U.S. DOE Project, Oct. 1984. AS19-80BC10310

Morrow N R, Chatzis I and Taber J J. Entrapment and mobilization of residual oil in bead packs. SPE Reservoir Engineering. 1988. 3(3): 927-934 (paper SPE 14423)

Ohen H A, Nnabuihe L, Felber B J, et al. A systematic laboratory core and fluid analysis program for the design of a cost effective treatment and cleanup guidelines for a produced water disposal scheme. Paper SPE 35369 presented at SPE/DOE Improved Oil Recovery Symposium, Apr. 21-24, 1996, Tulsa, Oklahoma

Pang S and Sharma M M. A model for predicting injectivity decline in water-injection wells. SPE Formation Evaluation. 1997. 12(3): 194-201 (paper SPE 28489)

Perkins T K and Johnston O C. A review of diffusion and dispersion in porous media. SPE Journal. 1963. 3(1): 70-84 (paper SPE 480)

Perkins T K and Johnston O C. A study of immiscible fingering in linear models. SPE Journal. 1969. 9(1): 39-46 (paper SPE 2230)

Ramakrishnan T S and Wasan D T. The relative permeability function for two-phase flow in porous media: effect of capillary number. Paper SPE 12693 presented at SPE Enhanced Oil Recovery Symposium, Apr. 15-18, 1984, Tulsa, Oklahoma

Rege S D and Fogler H S. A network model for deep bed filtration of solid particles and emulsion drops. AIChE Journal. 1988. 34(11): 1761-1772

Romero M I, Carvalho M S, Alvarado V, et al. Experiments and network model of flow of oil-water emulsion in porous media. Physical Review. 2011. E(84). 046305-1-7

Rousseau D, Latifa H and Nabzar L. Injectivity decline from produced-water reinjection: new insights on in-depth particle-deposition mechanisms. SPE Production & Operations. 2008. 23(4): 525-531 (paper SPE 107666)

Saripalli K P, Sharma M M and Bryant S L. Modeling injection well performance during deep-well injection of liquid wastes. Journal of Hydrology. 2000. 227(1-4): 41-55

Satter A, Shun Y M, Adams W T, et al. Chemical transport in porous media with dispersion and rate-controlled adsorption. SPE Journal. 1980. 20(3): 129-138 (paper SPE 6847)

Schlumberger. Eclipse Technical Description. Feb. 2007

Schmidt D P, Soo H and Radke C J. Linear oil displacement by the emulsion entrapment process. SPE Journal. 1984. 24(3): 351-360 (paper SPE 11333)

Schramm L L. Emulsions: Fundamentals and Applications in the Petroleum Industry. American Chemical Society. Vol. 231, May. 1992

Sheng J J. Modern Chemical Enhanced Oil Recovery: Theory and Practice. Elsevier: Gulf Professional Publishing. 2011

Soo H and Radke C J. The flow mechanism of dilute, stable emulsions in porous media. Ind. Eng. Chem. Fundamen. 1984a. 23 (3): 342-347

Soo H and Radke C J. Velocity effects in emulsion flow through porous media. Journal of Colloid and Interface Science. 1984b. 102(2): 462-476

Soo H and Radke C J. A filtration model for the flow of dilute stable emulsions in porous media —I. theory. Chemical Engineering Science. 1986. 41(2): 263-272

Soo H, Williams M C and Radke C J. A filtration model for the flow of dilute stable emulsions in porous media —II. parameter evaluation and estimation. Chemical Engineering Science. 1986. 41(2): 273-281

Spielman L A and Su Y P. Coalescence of oil-in-water suspensions by flow through porous media. Ind. Eng. Chem. Fundamen. 1977. 16(2): 272-282

Vaz A S L Jr., Bedrikovetsky P, Furtado C, et al. Effects of residual oil on reinjection of produced water. Paper SPE 100341 presented at SPE Europec/EAGE Annual Conference and Exhibition, Jun. 12-15, 2006, Vienna, Austria

Veil J A and Clark C E. Produced water volumes and management practices in the United States. Report for U.S. DOE, National Energy Technology Laboratory, Sept. 2009. DE-AC02-06CH11357

Veil J A and Quinn J J. Downhole separation technology performance: relationship to geologic conditions. Report for U.S. DOE, National Energy Technology Laboratory, Nov. 2004. W-31-109-Eng-38

Wang K L, Liang S C and Wang C C. Research of improving water injection effect by using active SiO_2 nano-powder in the low-permeability oilfield. Advanced Materials Research. 2010. 92: 207-212

Xu Z, Cai J G and Pan B C. Mathematically modeling fixed-bed adsorption in aqueous systems. Journal of Zhejiang University SCIENCE A. 2013. 14(3): 155-176

Yadava R R, Vinda R R and Kumar N. One-dimensional dispersion in unsteady flow in an adsorbing porous medium: an analytical solution. Hydrological Processes. 1990. 4: 189-196

Zhang N S, Somerville J M, Todd A C, et al. An experimental investigation of the formation damage caused by produced oily water injection. Paper SPE 26702 presented at the Offshore Europe, Sept. 7-10, 1993, Aberdeen, United Kingdom

(Edited by Sun Yanhua)